J. Phys. B: At. Mol. Opt. Phys. **33** (2000) 809–819. Printed in the UK PII: S0953-4075(00)07391-0

Electron-impact excitation of Rydberg and valence electronic states of nitric oxide: II. Integral cross sections

M J Brunger†§, L Campbell†, D C Cartwright‡, A G Middleton†, B Mojarrabi† and P J O Teubner†

† Department of Physics, The Flinders University of South Australia, GPO Box 2100, Adelaide, SA 5001, Australia

‡ Theoretical Divisions, B285, Los Alamos National Laboratories, Los Alamos, NM 87545, USA

Received 2 September 1999, in final form 11 November 1999

Abstract. Integral cross sections (ICSs) for the excitation of 18 excited electronic states, and four composite excited electronic states, in nitric oxide (NO) have been determined for incident electron energies of 15, 20, 30, 40 and 50 eV. These ICSs were derived by extrapolating the respective measured differential cross sections (M J Brunger *et al* 2000 *J. Phys. B: At. Mol. Opt. Phys.* **33** 783) to 0° and 180° and by performing the appropriate integration. Comparison of the present ICSs with the results of those determined in earlier optical emission measurements, and from theoretical calculations is made. At each incident energy considered, the current ICSs are also summed along with the corresponding elastic and rovibrational excitation ICSs from B Mojarrabi *et al* (1995 *J. Phys. B: At. Mol. Opt. Phys.* **28** 487) and the ionization cross sections from Rapp and Englander-Golden (1965 *J. Chem. Phys.* **43** 1464), to derive an estimate of the grand total cross sections (GTSs) for e^- + NO scattering. The GTSs derived in this manner are compared with the results from independent linear transmission experiments and are found to be entirely consistent with them. The present excited electronic state ICS, and those for elastic and rovibrational excitation from Mojarrabi *et al*, appear to represent the first set of self-consistent cross sections for electron impact scattering from NO.

1. Introduction

The rationale, from both fundamental and applied perspectives, for the importance of studying electron–nitric-oxide (NO) scattering processes was discussed in the companion paper [1] to this study and is not repeated here in the same detail. Briefly, however, there are two main reasons why the integral cross sections (ICSs) we have derived from our differential cross section (DCS) measurements [1] are expected to be useful. Firstly, the ICSs provide another test for the accuracy of electron–diatomic-molecule scattering theory calculations. While such a test is not as stringent as that afforded by the DCS measurements [1], it nonetheless is an important one. Secondly, the cross sections are very important in the modelling of many applied phenomena, including plasma etch processes, environmental and climate issues and the atmosphere. In particular, Cartwright *et al* [2] have recently used a subset of the ICSs we present here to model the behaviour of aurorae in which NO is an important constituent. Significant physical quantities such as relative number densities, volume emission rates, and metastable state number densities were presented in their analysis [2].

§ Present address: Department of Physics and Astronomy, University College London, Gower Street, London WC1E 6BT, UK.

0953-4075/00/040809+11$30.00

The only experimental e^-+ NO ICS data currently available in the literature are the emission ICSs due to Skubenich *et al* [3] and Schappe *et al* [4], and a preliminary report of some aspects of the present work [5]. The emission measurements of Skubenich *et al* reported ICSs for excitation of the $A\,^2\Sigma^+$, $B\,^2\Pi_r$, $b\,^4\Sigma^-$, $B'\,^2\Delta$ and $F\,^2\Delta$ electronic states from threshold to typically 50 eV, while that of Schappe *et al* was a single preliminary ICS measurement at 30 eV for the $B\,^2\Pi_r$ electronic state. In both cases we note these authors attempted to correct for possible cascade contributions to their data [3, 4]. From a theoretical perspective, the only available ICS results are from the distorted wave (DW) calculations of Machado *et al* [6], for electron-impact excitation of the $A\,^2\Sigma^+$, $C\,^2\Pi$ and $D\,^2\Sigma^+$ electronic states.

In the next section of this paper we discuss how we calculated the ICSs from our DCS measurements [1] and, in particular, our extrapolation procedure. Our results and a discussion of these results are then given in section 3, while in section 4 some conclusions are drawn.

2. Calculation of ICSs

The procedure for deriving ICSs from DCS data [1] is, in principle, quite straightforward. Initially, the measured DCSs are extrapolated to 0° and 180°. This extrapolation to forward and backward angles was typically performed with a method developed by Buckman and colleagues [7, 8], and it relies on a theoretical DCS for the relevant process and energy, of accurate shape. It is arguable (see Brunger *et al* [1]) that such theoretical cross sections do exist for a small subset ($n = 3$ members) of some of the Rydberg electronic states and a full discussion of the spectroscopy of NO is provided in [1]. However, as noted in [1], it was also quite apparent that the shapes of the experimental DCSs for the higher-order ($n = 4, 5, 6 \ldots$) Rydberg states in the $ns\sigma$, $np\pi$ etc series are very similar to those of the respective $n = 3$ members. Consequently, we were able to use the shape of the theory for the various $n = 3$ members as an extrapolation guide for the higher-order members of the corresponding series of states. Nonetheless such a procedure is intrinsically less certain than if the actual measured cross section data were available, and this additional uncertainty is reflected in the errors we quote on our derived ICSs (see tables 1–3). We note that the shape of the theory [6] we employed to aid us in our extrapolation to 0° used Born scattering amplitudes for the higher-order channels. We further note that it is these higher-order channels that largely determine the very forward angle behaviour of the theory DCS in this case. Where no theory was available for angular extrapolation, as in the case for the valence electronic states, three techniques were employed. In the first a 'by eye' procedure was adopted, while in the second a polynomial fit was made to the measured DCS and then the functional form of this fit was employed to extrapolate the data to 0° and 180°. Finally, the molecular phase shift analysis technique of Boesten and Tanaka [21], which is the most physically based of the three procedures, was applied. We note that in all cases the results from the application of these three techniques were checked for consistency. In addition, the sensitivity of the value of the integral (see equation (1) below) to the type of extrapolation procedure was investigated and this sensitivity is reflected in the errors we quote on our ICSs. Fortunately, most of the NO electronic state DCSs are strongly peaked in the forward direction [1] so the contribution to the integral of equation (1*a*) from the unaccessed angular regions greater than 90° is generally small.

Having performed the angular extrapolation to 0° and 180° the integral,

$$I_i(E_0) = \int_0^\pi (\mathrm{DCS}(E_0, \theta))_i \sin\theta \, \mathrm{d}\theta \tag{1a}$$

was evaluated at each E_0 for each electronic-state excitation process i using Simpson's rule.

Table 1. ICSs ($\times 10^{-19}$ cm^2) for electron-impact excitation of the Rydberg states of NO. The uncertainty on the data is also shown.

Rydberg state	ICS ($\times 10^{-19}$ cm^2) E_0 (eV)				
	15	20	30	40	50
$A\,^2\Sigma^+$	12.23 ± 4.28	14.83 ± 4.89	20.15 ± 6.04	17.59 ± 5.45	12.33 ± 4.32
$E\,^2\Sigma^+$	2.27 ± 1.47	2.67 ± 1.68	3.37 ± 2.02	3.93 ± 2.36	2.66 ± 1.65
$S\,^2\Sigma^+$	4.11 ± 2.26	8.76 ± 4.64	15.35 ± 7.67	10.47 ± 5.24	6.68 ± 3.41
$C\,^2\Pi_r$	23.10 ± 6.24	32.74 ± 8.18	41.32 ± 9.50	46.77 ± 10.76	32.69 ± 8.50
$K\,^2\Pi$	6.73 ± 2.56	8.09 ± 2.91	16.29 ± 5.54	18.90 ± 6.43	10.32 ± 3.72
$Q\,^2\Pi$	4.71 ± 2.03	6.63 ± 2.72	12.13 ± 4.85	14.63 ± 5.85	9.18 ± 3.86
$D\,^2\Sigma^+$	14.40 ± 5.04	18.53 ± 6.12	25.37 ± 7.61	29.68 ± 9.20	21.99 ± 7.48
$M\,^2\Sigma^+$	4.22 ± 1.81	5.63 ± 2.31	9.70 ± 3.88	10.56 ± 4.22	6.28 ± 2.64
$H'\,^2\Pi$	4.22 ± 2.40	5.89 ± 3.35	6.92 ± 3.67	9.32 ± 4.94	5.90 ± 3.30
$H\,^2\Sigma^+$	5.75 ± 3.28	8.70 ± 4.70	13.80 ± 7.18	13.67 ± 6.83	8.38 ± 4.61
$F\,^2\Delta$	4.40 ± 2.02	6.07 ± 2.67	9.29 ± 4.09	12.82 ± 5.51	8.00 ± 3.60
$N\,^2\Delta$	2.55 ± 2.99	—	5.30 ± 5.30	5.84 ± 5.84	5.64 ± 5.07
$O'\,^2\Pi + O\,^2\Sigma^+$	4.64 ± 2.13	6.49 ± 2.99	15.36 ± 6.60	13.06 ± 5.49	8.69 ± 3.82
$W\,^2\Pi + Y\,^2\Sigma^+$	9.43 ± 3.39	13.40 ± 4.42	22.70 ± 6.81	21.74 ± 6.52	13.36 ± 4.28
$T\,^2\Sigma^+ + U\,^2\Delta + 5f$	1.53 ± 0.99	2.31 ± 1.46	4.72 ± 2.83	4.34 ± 2.60	1.74 ± 1.06
$Z\,^2\Sigma^+ + 6d\delta + 6f$	0.98 ± 0.68	1.10 ± 0.75	2.11 ± 1.37	1.53 ± 0.99	1.51 ± 0.98

Table 2. ICSs ($\times 10^{-19}$ cm^2) for electron-impact excitation of the valence states of NO. The uncertainty on the data is also shown.

Valence state	ICS ($\times 10^{-19}$ cm^2) E_0 (eV)				
	15	20	30	40	50
$a\,^4\Pi$	7.63 ± 4.96	9.83 ± 6.19	13.51 ± 8.79	9.49 ± 6.17	6.74 ± 4.25
$b\,^4\Sigma^-$	47.12 ± 21.21	46.53 ± 22.80	41.37 ± 18.61	19.64 ± 9.23	9.40 ± 4.61
$B\,^2\Pi$	11.86 ± 6.64	14.99 ± 8.24	21.26 ± 11.27	14.66 ± 8.50	12.39 ± 7.43
$L'\,^2\Phi$	27.29 ± 15.56	22.96 ± 14.23	18.37 ± 10.10	21.16 ± 11.00	20.27 ± 11.56
$B'\,^2\Delta$	32.45 ± 11.36	65.26 ± 21.54	84.19 ± 25.26	57.76 ± 17.91	21.58 ± 7.34
$L\,^2\Pi$	36.06 ± 15.15	54.68 ± 20.78	118.49 ± 45.03	139.26 ± 54.31	118.46 ± 49.76

The ICS ($Q_i(E_0)$) for excitation to state i is then evaluated in the usual fashion using

$$Q_i(E_0) = 2\pi\, I_i(E_0). \tag{1b}$$

The overall errors on the present ICSs, as quoted in absolute terms in tables 1 and 2, were determined from the quadrature sum of the uncertainty in each angular extrapolation for process i and energy E_0, and an uncertainty due to the errors on the DCS measurements, again for each process i and energy E_0.

3. Results and discussion

ICSs for excitation of the $A\,^2\Sigma^+$, $E\,^2\Sigma^+$, $S\,^2\Sigma^+$, $C\,^2\Pi_r$, $K\,^2\Pi$, $Q\,^2\Pi$, $D\,^2\Sigma^+$, $M\,^2\Sigma^+$, $H'\,^2\Pi$, $H\,^2\Sigma^+$, $F\,^2\Delta$ and $N\,^2\Delta$ Rydberg electronic states, $O'\,^2\Pi + O\,^2\Sigma^+$, $W\,^2\Pi + Y\,^2\Sigma^+$, $T\,^2\Sigma^+ + U\,^2\Delta + 5f$ and $Z\,^2\Sigma^+ + 6d\delta + 6f$ composite Rydberg electronic, and $a\,^4\Pi$, $b\,^4\Sigma^-$, $B\,^2\Pi$, $L'\,^2\Phi$, $B'\,^2\Delta$ and $L\,^2\Pi$ valence electronic states in NO have been determined. The present

Table 3. GTSs ($\times 10^{-16}$ cm^2) for electron scattering from NO. Figures in parentheses indicate the absolute uncertainty expressed as a percentage: (a) Mojarrabi *et al* [13], (b) Rapp and Englander-Golden [14] and (c) Szmytkowski and Maciag [15].

	GTS ($\times 10^{-16}$ cm^2)						
E_0 (eV)	(a) Q_{elastic}	(a) $Q_{0\rightarrow 1}$	(a) $Q_{0\rightarrow 2}$	$\sum_{\text{all states}} Q_{\text{electronic}}$	(b) $Q_{\text{ionization}}$	$Q_{\text{GTS}}^{\text{present}}$	(c) Q_{GTS}
1.5	10.473 (30)	—	—	—	—	10.473 (30)	12.3 (5)
3.0	9.604 (30)	—	—	—	—	9.604 (30)	9.45 (3)
5.0	9.239 (20)	—	—	—	—	9.239 (20)	9.22 (3)
7.5	9.095 (20)	0.028 (25)	—	—	—	9.123 (25)	9.52 (3)
10.0	9.241 (20)	0.074 (25)	0.014 (30)	—	0.018 (10)	9.347 (25)	10.1 (3)
15.0	9.714 (20)	0.270 (25)	0.073 (30)	0.270 (50)	0.418 (10)	10.745 (30)	11.5 (3)
20.0	9.707 (20)	0.097 (25)	0.022 (30)	0.346 (47)	0.813 (10)	10.985 (30)	11.4 (3)
30.0	9.314 (20)	0.022 (25)	—	0.521 (43)	1.522 (10)	11.379 (30)	10.8 (3)
40.0	8.214 (20)	0.014 (25)	—	0.497 (45)	2.086 (10)	10.811 (30)	10.3 (3)
50.0	6.444 (20)	—	—	0.344 (48)	2.482 (10)	9.270 (30)	9.6 (3)

study determined these ICSs for electrons with incident energy 15, 20, 30, 40 and 50 eV, respectively, and are tabulated, along with their absolute uncertainty, in tables 1 and 2. This work clearly represents a significant number of data that is too large to be graphically presented in this section for every state. Consequently, only plots for those excited electronic states that we choose to highlight are given here, with these states largely being chosen on the basis of the availability of other data [3, 4] and/or calculations [6], against which we can compare the present results.

3.1. $A\,^2\Sigma^+$ Rydberg state (excitation energy = 5.484 eV)

In table 1 we present our ICSs for electron-impact excitation of the $A\,^2\Sigma^+$ Rydberg electronic state. The present data are also plotted graphically in figure 1, where they are compared with the earlier emission ICS results of Skubenich *et al* [3] and the DW theory calculation results of Machado *et al* [6]. It is clear from figure 1 that the theoretical results overestimate the magnitude of the ICSs over the entire common energy range. Indeed, while the results of Machado *et al* [6] do appear to converge towards the experimental values at higher energies, consistent with what we saw previously for the corresponding DCSs [1], at lower energies the calculated ICSs do not appear to exhibit the correct threshold behaviour. On the other hand, the measurements of Skubenich *et al* [3] are, in general, in fair accord with the present ICSs in terms of both the shape and magnitude of the cross section. While we note from figure 1 that there are some differences in detail between the magnitudes of the two experimental ICSs, these may simply have resulted from the cascade correction of Skubenich *et al* being somewhat inexact. Thus we can conclude that the present ICS for the $A\,^2\Sigma^+$ state largely confirms the result of Skubenich *et al*, and that therefore the magnitude of the $A\,^2\Sigma^+$ ICS is one to two orders of magnitude smaller than that for the corresponding (in terms of energy loss) state of N_2. Clearly, more theoretical work into an explanation for the origin of this latter observation is required.

3.2. $C\,^2\Pi_r$ Rydberg state (excitation energy = 6.499 eV)

Unlike the $A\,^2\Sigma^+$ state, there is no independent measurement against which we can compare our ICS for the electron-impact excitation of the $C\,^2\Pi_r$ Rydberg electronic state. In this case

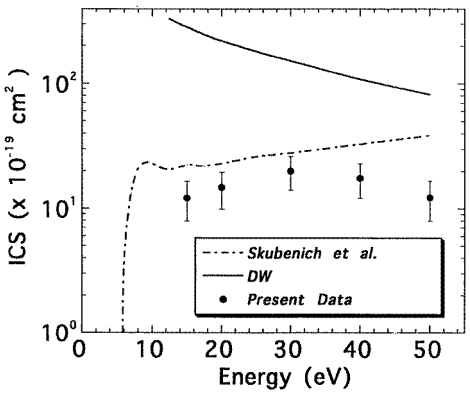

Figure 1. ICSs ($\times 10^{-19}$ cm^2) for the electron-impact excitation of the A $^2\Sigma^+$ electronic state. The present data (●) are compared with the emission results of Skubenich *et al* [3] (— · —) and the DW calculation results of Machado *et al* [6] (——).

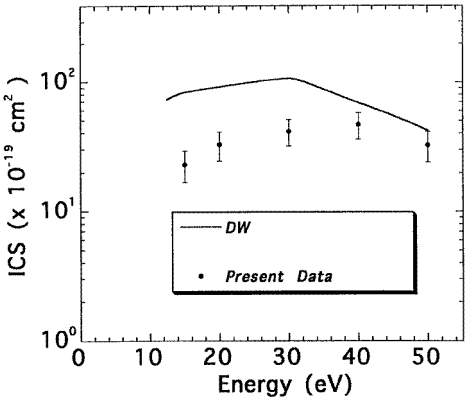

Figure 2. ICSs ($\times 10^{-19}$ cm^2) for the electron-impact excitation of the C $^2\Pi$ electronic state. The present data (●) are compared with the DW calculation results of Machado *et al* [6] (——).

we can only compare the present data with the DW calculation result of Machado *et al* [6]. This is done in figure 2, with tabulated values of the current C $^2\Pi_r$ cross sections also being found in table 1. The theoretical ICS for the C $^2\Pi_r$ state seriously overestimates the magnitude of this ICS at lower energies (see figure 2), but at 50 eV the calculated and present ICSs are in quite good agreement, at least to within the experimental uncertainty. Contrary to the situation we found for the A $^2\Sigma^+$ state, the functional form (shape) of the theoretical and experimental C $^2\Pi_r$ ICSs are in reasonably good accord. In addition, it is also worth noting that the discrepancy between the DW theory and present results, in terms of the magnitude of the cross sections, is less extreme for the C $^2\Pi_r$ state than for the A $^2\Sigma^+$ state. Whether these results indicate that the DW theory is more exact in describing $^2\Pi_r \rightarrow {}^2\Pi_r$ excitation processes in comparison with the $^2\Pi_r \rightarrow {}^2\Sigma^+$ excitation processes, or whether it is because the C $^2\Pi_r$ wavefunction used by Machado *et al* [6] provides a more realistic description of that state than that afforded by their A $^2\Sigma^+$ wavefunction for the A $^2\Sigma^+$ state, is unclear at this time.

3.3. F $^2\Delta$ Rydberg state (excitation energy = 7.722 eV)

The F $^2\Delta$ state is the $n = 3$ member of the $n\,\mathrm{d}\delta$ Rydberg series of excited electronic states in NO. The current ICSs for this state are summarized in table 1 and these data, and the photon-emission data of Skubenich *et al* [3], are plotted in figure 3. Note that there is at present no theory for electron-impact excitation of the F $^2\Delta$ state against which we can compare the two sets of available ICS experimental measurements.

From the comparison in figure 3, it is apparent that there is very good agreement, across the entire common energy range of measurement, between the present ICS and that of Skubenich *et al*. This statement is valid in terms of both the shape and magnitude of the F $^2\Delta$ ICS where, with the exception of the datum point at 40 eV, the present results overlap those of Skubenich *et al*, to within our quoted errors. However, we consider that such a high level of agreement is probably somewhat fortuitous, given the difficulty Skubenich *et al* [3] must have had in applying an accurate cascade correction to their measured photon flux.

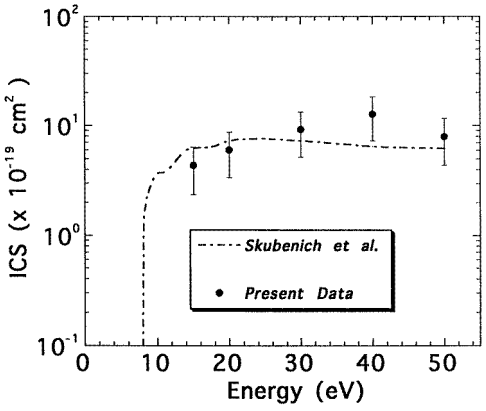

Figure 3. ICSs ($\times 10^{-19}$ cm^2) for the electron-impact excitation of the F $^2\Delta$ electronic state. The present data (●) are compared with the emission results of Skubenich *et al* [3] (— · —).

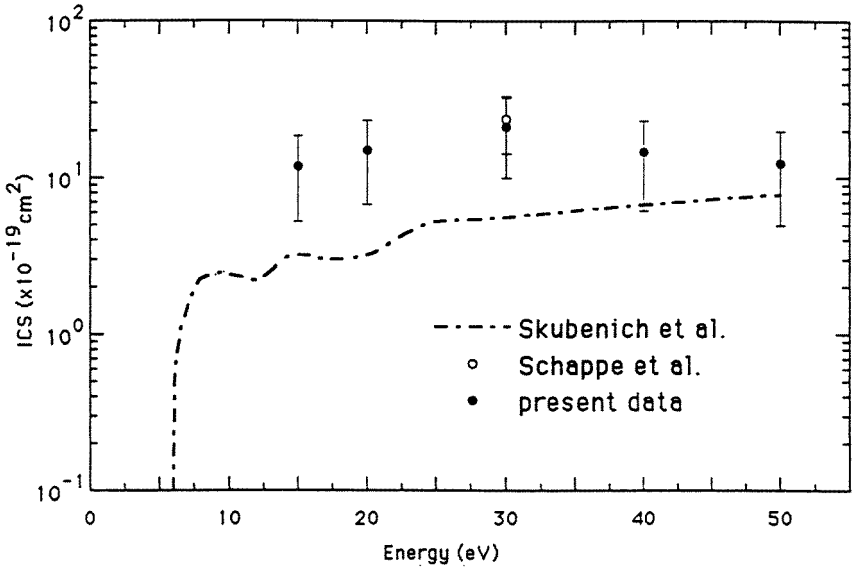

Figure 4. ICSs ($\times 10^{-19}$ cm^2) for the electron-impact excitation of the B $^2\Pi$ electronic state. The present data (●) are compared with the emission results of Skubenich *et al* [3] (— · —) and Schappe *et al* [4] (○).

3.4. B $^2\Pi_r$ *valence state (excitation energy = 5.769 eV)*

In table 2 we present our ICSs for electron-impact excitation of the B $^2\Pi_r$ valence electronic state. The present data are also plotted graphically in figure 4, where they are compared with the emission ICS results of Skubenich *et al* [3] and Schappe *et al* [4]. Note that there are no theoretical ICS data against which we can compare the experimental results, as is true for all the NO valence states. It is clear from figure 4 that the present ICSs are, in general, larger in magnitude, across the entire common energy range, than the corresponding ICSs from Skubenich *et al* [3]. This discrepancy may be due to either overcorrection for cascades or a problem with their normalization technique. The ICS of Skubenich *et al* exhibits structure for electron energies between approximately 9–20 eV which the current measurements, due to their widely spaced energy grid of measurement, could not crosscheck. However, resonance effects, due to the decay of Feshbach resonances, have been observed in this energy range in

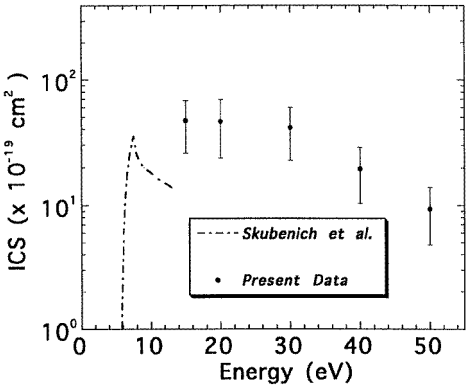

Figure 5. ICSs ($\times 10^{-19}$ cm^2) for the electron-impact excitation of the $b^4\Sigma^-$ electronic state. The present data (●) are compared with the emission results of Skubenich *et al* [3] (— · —).

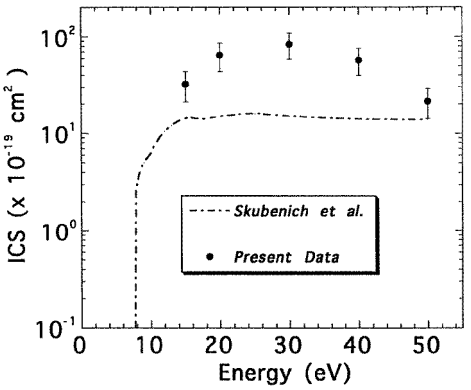

Figure 6. ICSs ($\times 10^{-19}$ cm^2) for the electron-impact excitation of the $B'^2\Delta$ electronic state. The present data (●) are compared with the emission results of Skubenich *et al* [3] (— · —).

transmission spectroscopy by Sanche and Schulz [9] and in high-resolution experiments by Gresteau *et al* [10–12]. Consequently, it is possible that the structure in the ICS of Skubenich *et al* is physical. A very recent emission ICS for electron-impact excitation of the $B^2\Pi_r$ electronic state, at the single electron energy of 30 eV, was reported by Schappe *et al* [4]. Although the measurement of Schappe *et al* is still preliminary, it is in excellent agreement with the current result (see figure 4).

3.5. $b^4\Sigma^-$ valence state (excitation energy = 5.718 eV)

The present ICSs for the $b^4\Sigma^-$ state are shown in figure 5, along with the data from Skubenich *et al* [3]. Skubenich *et al* were restricted, in this case, to electron energies less than about 12 eV in their ICSs, after which cascade contributions became dominant thereby ruling out further measurements. Because our ICSs begin at 15 eV, it is obvious that the present results and those of Skubenich *et al* do not overlap in energy. However, the trend in the magnitudes of their respective cross sections is encouraging, suggesting that we can anticipate no significant discrepancy between these ICSs for the two measurements. We note that the errors on our $b^4\Sigma^-$ ICSs, at each energy studied, are significantly larger than the uncertainties for the $A^2\Sigma^+$ and $C^2\Pi_r$ ICSs. This is simply due to the shapes of the $b^4\Sigma^-$ DCSs at small scattering angles (see [1]), which results in the ICS being particularly sensitive to the type of angular extrapolation technique adopted, which in turn is reflected in the uncertainties on the results for the $b^4\Sigma^-$ state that we quote in table 2.

3.6. $B'^2\Delta$ valence state (excitation energy = 7.442 eV)

The level of agreement between the present ICSs for the electron-impact excitation of the $B'^2\Delta$ state and those reported by Skubenich *et al* [3] is, with the exception of the datum point at 50 eV, in general quite poor, as is shown in figure 6. We can see from figure 6 that the present data are greater in magnitude than those of Skubenich *et al*, with the discrepancy between them at 30 eV being almost a factor of 5. In addition, whereas the shape of the ICS of Skubenich *et al*, above 15 eV, is almost constant with energy, the present ICS has a clear, almost inverted parabola, energy dependence. While the mismatch in absolute values between the two data

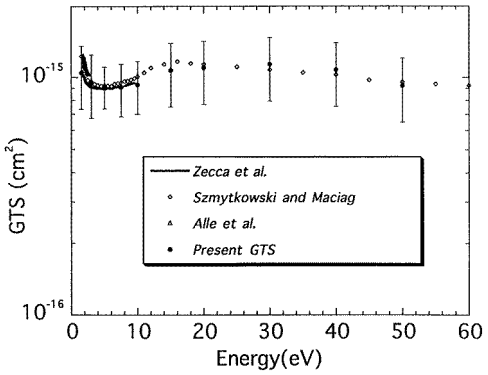

Figure 7. GTSs ($\times 10^{-16}$ cm^2) for e$^-$+ NO scattering. The present data (●) are compared with the other experimental determinations of Zecca *et al* [16] (——), Szmytkowski and Maciag [15] (◇) and Alle *et al* [17] (△).

sets could again, at least in part, be due to a normalization problem with the optical result [3], the reason for the discrepancy between the shapes is not known. One reasonable possibility is that as the cascade correction is energy dependent, then any error in it could obscure the actual energy dependent shape. Tabulated values for our $B'^2\Delta$ ICSs can be found in table 2.

3.7. Grand total cross sections (GTSs)

Summing the ICSs for all electronic states and adding this sum to the corresponding elastic and rovibrational ICSs of Mojarrabi *et al* [13] and the ionization cross sections of Rapp and Englander-Golden [14] results in a quantity that can be directly compared with the GTS. That is

$$Q_{\rm GTS}^{\rm present}(E_0) = Q_{\rm elastic}^{[13]}(E_0) + \sum_{i=1}^{2} Q_{0\to i}^{\rm vibrational[13]}(E_0) + \sum_{\rm all\ states} Q_{\rm electronic}^{\rm present}(E_0) + Q_{\rm ionization}^{[14]}(E_0). \quad (2)$$

In the course of this work we discovered that there had been an error made by Mojarrabi *et al* [13] in the integration of their elastic DCS. Their values [13] for $Q_{0\to i}^{\rm vibrational}$, however, stand. The correct values for the elastic ICS of Mojarrabi *et al* are therefore now given in table 3, along with the appropriate values of $Q_{0\to i}^{\rm vibrational}(E_0)$, $\sum_{\rm all\ states} Q_{\rm electronic}^{\rm present}(E_0)$, $Q_{\rm ionization}(E_0)$ and the $Q_{\rm GTS}^{\rm present}(E_0)$. Also included in table 3 are the values of the GTS for e$^-$+ NO scattering as measured by Szmytkowski and Maciag [15]. The rationale behind our calculation of $Q_{\rm GTS}^{\rm present}(E_0)$ is that it allows us to cross check the self-consistency of our present electronic state ICSs, and our earlier elastic and rovibrational ICSs, against the results of accurate, independent measurements of the GTS using linear transmission techniques. The result of this comparison is best illustrated in figure 7 where the present GTSs are compared with the results of Zecca *et al* [16], Szmytkowski and Maciag [15] and Alle *et al* [17]. It is apparent from a consideration of figure 7 that over the entire common energy range of measurement, the present GTSs are in very good agreement with the linear transmission measurement results [15–17], some of which also employed time-of-flight techniques.

It is clear from table 3 that the dominant contribution to the GTS, at all energies below and including 50 eV, is from elastic scattering. Indeed, excitation of the electronic states contributes only about 2% to the GTS at 15 eV and 5% to the GTS at 30 eV. In their recent review Zecca *et al* [18] estimated what they thought the electronic state excitation contribution to the GTS for e$^-$+ NO scattering should be. Their estimates are confirmed by the present measurements.

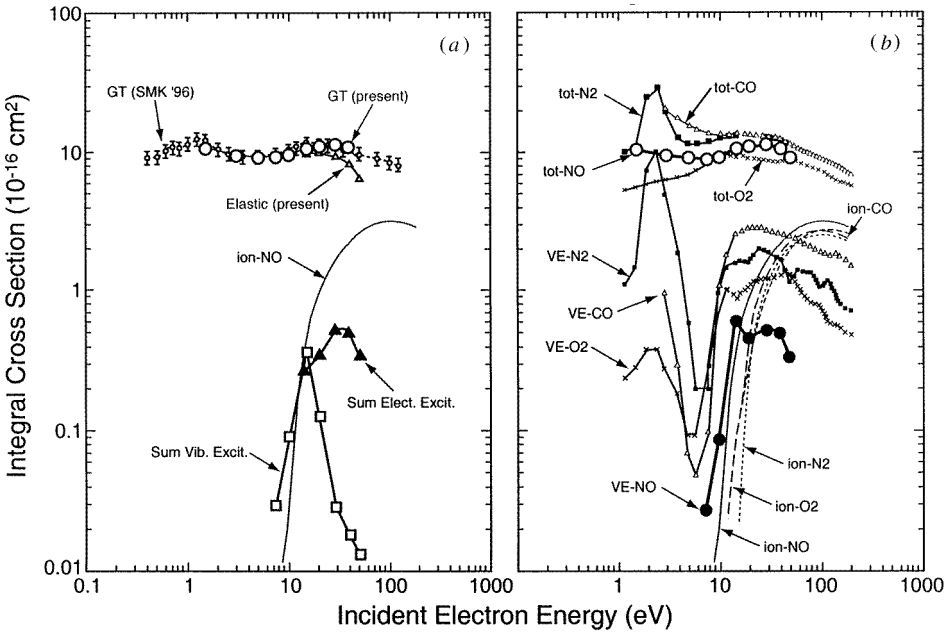

Figure 8. (*a*) The GTS for NO derived from the present work (GT(present)) compared with the same quantity measured directly by Szmytkowski and Maciag (SMK '96) [15]. For comparison, the total ionization (ion-NO) [14], present results for elastic electron scattering by NO, and present results for vibrational + electronic excitations are also shown. (*b*) The grand total (tot-xx) [15,20], total ionization (ion-xx)[14], and vibrational + electronic (VE-xx) [20] ICSs for the four diatomic molecules xx = CO, NO, O_2 and N_2. New results from this study for NO GTS and NO vibrational + electronic excitation ICS are indicated by the large open and closed circles, respectively. This comparison is to put the shape and magnitude of the new NO GTS and ICS from this study into quantitative perspective with respect to the analogous cross sections for CO, O_2 and N_2.

4. Conclusions

We have reported an extensive set of ICSs for the electron-impact excitation of the Rydberg and valence electronic states of NO. Agreement of the present data with the earlier optical emission results of Skubenich *et al* was patchy. In some cases, such as for the $F\,^2\Delta$ state, we would characterize the overall level of agreement as being good, while for others such as the $B'^2\Delta$ state the agreement is quite poor. On the other hand, the present $B\,^2\Pi_r$ ICS at 30 eV is in very good accord with the corresponding emission ICS of Schappe *et al*. In addition we have demonstrated that our electronic state ICSs, when combined with our earlier ICS measurements for elastic scattering and rovibrational excitation, are in very good agreement with accepted values of the GTS for e^-+ NO scattering. We therefore believe that this set of cross sections for elastic scattering, vibrational excitation and electronic-state excitation represents a self-consistent set which can be used by colleagues when they are attempting to model the behaviour of various physical phenomena in which NO plays a role [2, 19].

Finally, in figure 8, we present a comparison of the integral cross sections for various electron scattering processes (*a*) in NO and (*b*) for the four diatomic molecules: NO, CO, O_2 and N_2.

The GTSs for NO were taken from Szmytkowski and Maciag [15], and those for CO, N_2 and O_2 were taken from the compilation by Hayashi [20]. The integral total ionization cross

sections by electron impact for NO, CO, O_2 and N_2 were taken from Rapp and Englander-Golden [14]. The integral elastic scattering cross sections for CO, N_2 and O_2 were taken from Hayashi [20] and that for NO was taken from the work of Mojarrabi *et al* [13] (see also section 3.7). In order to have cross section values over the same set of incident electron energies, the cross sections for ionization and elastic scattering were linearly interpolated to the same set of energies used by Hayashi.

Using these GTSs and ICSs, estimates of the ICSs for all vibrational + electronic excitation by electron-impact, for each species, were obtained from

$$\sum (Q^{\text{vibrational}} + Q^{\text{electronic}}) = Q_{\text{GTS}} - Q_{\text{elastic}} - Q_{\text{ionization}} \tag{3}$$

where the quantity $\sum(Q^{\text{vibrational}} + Q^{\text{electronic}})$ is actually the sum of all inelastic scattering processes other than ionization. Note that while we have suppressed the notation, each of the terms in equation (3) is calculated at a given incident electron energy E_0.

Figure 8(*a*) again compares the GTS for NO derived from the present work with the same quantity measured directly by Szmytkowski and Maciag. In addition, however, the NO total ionization and $\sum_i Q_{0\to i}^{\text{vibrational}}$ and $\sum_{\text{all states}} Q_{\text{electronic}}$, from Mojarrabi *et al* [13] and the present work respectively, are also plotted for the purpose of comparison. Figure 8(*b*) compares the GTS, total ionization and $\sum(Q^{\text{vibrational}} + Q^{\text{electronic}})$ ICSs for the four diatomic molecules NO, CO, O_2 and N_2. The purpose of this comparison is to put the shapes and magnitudes of the total ICSs into quantitative perspective with respect to the GTSs for each molecule.

The following qualitative conclusions can be drawn from figure 8. As expected, the GTSs are similar for all four molecules in both magnitude and shape for electron energies greater than about 8 eV. This is generally true in spite of NO and CO possessing permanent dipole moments while N_2 and O_2 do not. The ionization cross sections are even more similar, at all energies, and it is noted that the NO ionization cross section is slightly larger than those for CO, N_2 and O_2. Perhaps most importantly, particularly in respect to our understanding of atmospheric and other practical phenomena where these four molecules play a role, the ICS for vibrational plus electronic excitation in NO is significantly smaller than that for the other diatomic molecules at electron energies above about 8 eV.

Acknowledgments

This work was supported by a grant from the Australian Research Council (ARC). MJB also thanks the ARC for his fellowship. The hospitality of Dr W R Newell and his colleagues at University College London is gratefully acknowledged by MJB.

References

[1] Brunger M J, Campbell L, Cartwright D C, Middleton A G, Mojarrabi B and Teubner P J O 2000 *J. Phys. B: At. Mol. Opt. Phys.* **33** 783
[2] Cartwright D C, Brunger M J, Campbell L, Mojarrabi B and Teubner P J O 1998 *Geophys. Res. Lett.* **25** 1495
[3] Skubenich V V, Povch M M and Zapesochnyi I P 1977 *High Energy Chem. (USSR)* **11** 92
[4] Schappe R S, Hall L and Wawrzyniak M 1997 *Bull. Am. Phys. Soc.* **42** 1710
[5] Mojarrabi B, Campbell L, Teubner P J O, Brunger M J and Cartwright D C 1996 *Phys. Rev.* A **54** 2977
[6] Machado L E, Monzani A L, Lee M-T and Fujimoto M M 1995 *Proc. Int. Symp. on Electron– and Photon–Molecule Collisions and Swarms* ed C W McCurdy and T Rescigno (Berkeley, CA: Lawrence Livermore Press) H32
[7] Buckman S J, Brunger M J, Newman D S, Snitchler G, Alston S, Norcross D W, Morrison M A, Saha B C, Danby G and Trail W K 1990 *Phys. Rev. Lett.* **65** 3253
[8] Alle D T, Gulley R J, Buckman S J and Brunger M J 1992 *J. Phys. B: At. Mol. Opt. Phys.* **25** 1533
[9] Sanche L and Schulz G J 1972 *Phys. Rev.* A **6** 69

[10] Gresteau F, Hall R I, Mazeau J and Vichon D 1977 *J. Phys. B: At. Mol. Phys.* **10** L545
[11] Gresteau F, Hall R I, Huetz A, Vichon D and Mazeau J 1979 *J. Phys. B: At. Mol. Phys.* **12** 2925
[12] Gresteau F, Hall R I, Huetz A, Vichon D and Mazeau J 1979 *J. Phys. B: At. Mol. Phys.* **12** 2937
[13] Mojarrabi B, Gulley R J, Middleton A G, Cartwright D C, Teubner P J O, Buckman S J and Brunger M J 1995 *J. Phys. B: At. Mol. Opt. Phys.* **28** 487
[14] Rapp D and Englander-Golden D 1965 *J. Chem. Phys.* **43** 1464
[15] Szmytkowski C and Maciag K 1991 *J. Phys. B: At. Mol. Opt. Phys.* **24** 4273
[16] Zecca A, Lazzizzera I, Krauss M and Kuyatt C E 1974 *J. Chem. Phys.* **61** 4560
[17] Alle D T, Brennan M J and Buckman S J 1996 *J. Phys. B: At. Mol. Opt. Phys.* **29** L277
[18] Zecca A, Karwasz G P and Brusa R S 1996 *Riv. Nuovo Cimento* **19** 1
[19] Cartwright D C, Brunger M J, Campbell L and Teubner P J O 1999 *J. Geophys. Res.* submitted
[20] Hayashi M 1981 *Recommended Values of Transport Cross Sections for Elastic Collision and Total Cross Section for Electrons in Atomic and Molecular Gases* IPPJ-AM-19 (Nagoya Institute of Technology)
[21] Boesten L and Tanaka H 1991 *J. Phys. B: At. Mol. Opt. Phys.* **24** 821